LETTERS
PUBLISHED ONLINE: 18 APRIL 2016 | DOI: 10.1038/NCLIMATE2995
nature climate change

Regional disparities in the beneficial effects of rising CO_2 concentrations on crop water productivity

Delphine Deryng[1,2,3*], Joshua Elliott[1,2], Christian Folberth[4,5], Christoph Müller[6], Thomas A. M. Pugh[7,8], Kenneth J. Boote[9], Declan Conway[10], Alex C. Ruane[11,2], Dieter Gerten[6,12], James W. Jones[9], Nikolay Khabarov[5], Stefan Olin[13], Sibyll Schaphoff[6], Erwin Schmid[14], Hong Yang[4] and Cynthia Rosenzweig[11,2]

Rising atmospheric CO_2 concentrations ($[CO_2]$) are expected to enhance photosynthesis and reduce crop water use[1]. However, there is high uncertainty about the global implications of these effects for future crop production and agricultural water requirements under climate change. Here we combine results from networks of field experiments[1,2] and global crop models[3] to present a spatially explicit global perspective on crop water productivity (CWP, the ratio of crop yield to evapotranspiration) for wheat, maize, rice and soybean under elevated $[CO_2]$ and associated climate change projected for a high-end greenhouse gas emissions scenario. We find CO_2 effects increase global CWP by 10[0;47]%–27[7;37]% (median[interquartile range] across the model ensemble) by the 2080s depending on crop types, with particularly large increases in arid regions (by up to 48[25;56]% for rainfed wheat). If realized in the fields, the effects of elevated $[CO_2]$ could considerably mitigate global yield losses whilst reducing agricultural consumptive water use (4–17%). We identify regional disparities driven by differences in growing conditions across agro-ecosystems that could have implications for increasing food production without compromising water security. Finally, our results demonstrate the need to expand field experiments and encourage greater consistency in modelling the effects of rising $[CO_2]$ across crop and hydrological modelling communities.

Research indicates unabated climate change will exacerbate water scarcity around the world[4,5]. This is thought to threaten agricultural productivity and food security, especially in arid regions[6–8], where agriculture relies heavily on irrigation and consumes the majority of diverted freshwater[9]. Yet, rising atmospheric CO_2 concentrations ($[CO_2]$), despite directly contributing to climate change, have the potential to increase crop water productivity (CWP; defined here as the ratio of crop yield to total crop water use over the growing season) by enhancing photosynthesis and reducing leaf-level transpiration of plants[1,2]. If these effects can be harnessed to increase crop yields and reduce water consumption in agriculture at national to continental scales, this could greatly help in ensuring food and water security for a rapidly growing global population[10].

The enhancement of photosynthesis rates in C_3 crops and the reduction in stomatal conductance—and thus water loss—in both C_3 and C_4 crops under elevated $[CO_2]$ is well supported by numerous plant manipulation experiments[1,11]. The extent to which such mechanisms eventually enhance crop yields and reduce evapotranspiration (ET) is less well understood on large scales[12–14], but observations of crops grown under elevated $[CO_2]$ (Free Air Carbon Enrichment, FACE) show that an average increase of 13% in yields and 5% reduction in ET can be expected[1,15]. However, FACE experiments are for the most part located in temperate regions, whereas tropical and arid regions, where food security is most threatened[6], are under-represented[16,17]. Given the strong dependence of CO_2 effects on environmental conditions and the limited coverage of FACE experiments for representing the diversity of agricultural production systems worldwide[16,17], process-based modelling is needed to assess the scope of beneficial effects of elevated CO_2 on CWP[18]. The few such studies that exist rely on single models, for example, refs 19,20, and therefore do not cover the range of uncertainty embedded in crop modelling methodology, and particularly in calculations of the effect of rising $[CO_2]$ on yields of C_3 crops (for example, Fig. 4 in ref. 21), which can lead to substantial variation in simulated impacts, for example, refs 3,22.

Here we present a spatially explicit global assessment of effects of elevated $[CO_2]$ on future CWP originating from a large ensemble of simulations, resulting from a recent international modelling intercomparison exercise[3]. The model ensemble comprises six global gridded crop models (GGCMs), with simulations using

[1]Computation Institute, University of Chicago, Chicago, Illinois 60637, USA. [2]Center for Climate Systems Research, Columbia University, New York, New York 10025, USA. [3]Tyndall Centre for Climate Change Research, University of East Anglia, Norwich NR4 7TJ, UK. [4]Swiss Federal Institute of Aquatic Science and Technology (EAWAG), 8600 Dübendorf, Switzerland. [5]International Institute for Applied Systems Analysis (IIASA), Ecosystems Services and Management Program, Schlossplatz 1, Laxenburg A-2361, Austria. [6]Potsdam Institute for Climate Impact Research, 14473 Potsdam, Germany. [7]Karlsruhe Institute of Technology, IMK-IFU, 82467 Garmisch-Partenkirchen, Germany. [8]School of Geography, Earth and Environmental Science, University of Birmingham, Birmingham B15 2TT, UK. [9]University of Florida, Gainesville, Florida 32611-0500, USA. [10]Grantham Research Institute on Climate Change & the Environment, London School of Economics and Political Science, London WC2A 2AE, UK. [11]NASA Goddard Institute for Space Studies, New York, New York 10025, USA. [12]Geography Department, Humboldt-Universität zu Berlin, 10099 Berlin, Germany. [13]Department of Physical Geography and Ecosystem Science, Lund University, Lund SE-223 62, Sweden. [14]University of Natural Resources and Life Sciences, 1180 Vienna, Austria.
*e-mail: deryng@uchicago.edu

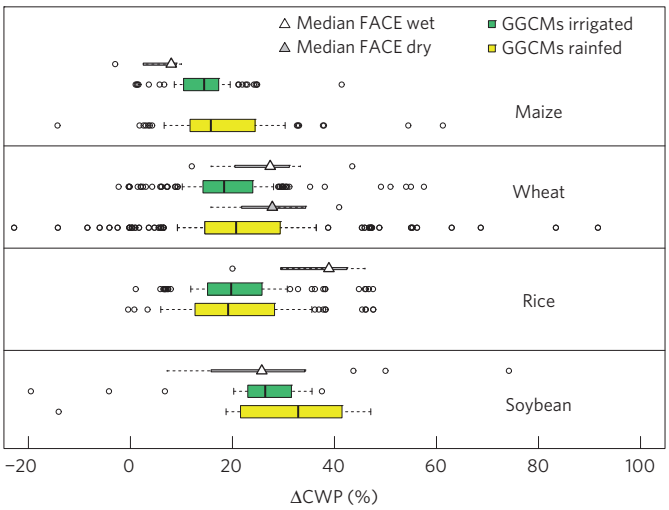

Figure 1 | Comparison between FACE observations and GGCM simulations. CWP responses to elevated [CO_2] (550 ppm from FACE and corresponding grid-cell values extracted from GGCM simulations in this study) for maize, wheat, rice and soybean at ample and limited soil water. FACE data were collected from references summarized in Supplementary Table 1. The left and right sides of the boxes are lower and upper quartiles, respectively, and the band near the middle of the boxes is the median value across each set of simulations. Open circles are outliers. Note rainfed simulations for maize and rice at the FACE locations correspond to negligible water stress conditions.

climate input data from five global climate models (GCMs)[23] under a high-end greenhouse gas emissions scenario that projects a doubling of [CO_2] by 2080 relative to 2000—namely, the Representative Concentration Pathway (RCP) 8.5 (ref. 24) (see Methods). We estimate changes in simulated crop yields, actual evapotranspiration (AET) and CWP under rising [CO_2] and associated climate change for three C_3 crops (wheat, rice and soybean) and one C_4 crop (maize) throughout the twenty-first century relative to the present-day baseline (approximately 2000). To assess the specific role of elevated [CO_2] under various crop growing conditions, we considered two sets of simulations: the first accounting for both effects of elevated [CO_2] and changes in climate (CC w/ CO_2); the second accounting for changes in climatic conditions whilst keeping [CO_2] constant to present-day levels (CC w/o CO_2). We examined rainfed and irrigated growing conditions according to the present distribution of rainfed and irrigated cropping areas[25] and assumed no change in the assumption of individual models on input rates of fertilizer applications (see Methods). We collected all available FACE data on both yield and water use and/or crop water use efficiency for the four crops (see Methods; Supplementary Tables 1 and 2) to compare simulated and observed CO_2 effects on CWP at elevated concentrations (Fig. 1 and Supplementary Results). We present and discuss in detail sources of differences in simulated CWP in the Methods.

By 2080 under CC w/o CO_2, we find severe negative impacts on crop yields at the global scale and small reductions in corresponding AET, which together lead to large reductions in global CWP (median 13–26%, with larger reductions for C_3 crops) supported by more than 80% of the simulations (Table 1; see Methods for a description of the aggregation approach). In contrast, under CC w/ CO_2, median negative impacts on yields are fully compensated for wheat and soybean, and mitigated by up to 90% for rice and 60% for maize. We find effects of elevated [CO_2] reduce the global AET of maize, wheat and soybean by a median 8–17%, but are less pronounced (3%) on AET of rice, as the latter is mostly grown under well-watered conditions, and thus less affected by water stress (Table 1 and Supplementary Table 3). The combined effects of CC w/ CO_2 on yield and AET result in substantial increases in global average CWP of wheat (27[7;37]%) and soybean (18[−9;42]%) and moderate increases in that of maize (13[3;22]%) and rice (10[0;47]%) (Table 1; numbers in square brackets represent the interquartile range).

We compare impacts across climatic regions and growing conditions. By 2080 under CC w/ CO_2, simulated CWP in arid, temperate and cold regions exhibits particularly large increases relative to 2000 (median increase above 15%), whereas CWP in tropical cropland increases by only a negligible amount on average (median increase below 4%) (Fig. 2). In fact, we find CWP of crops grown in arid climate benefit the most from the effects of elevated [CO_2], especially under rainfed conditions (Supplementary Table 3), leading to additional crop production along with substantial reductions in consumptive crop water use by 2080. For example, assuming wheat rainfed areas remain steady in the future, global production of rainfed wheat could increase by a median 9% by 2080 relative to 2000, whereas corresponding consumptive water use decreases by 11% (see Supplementary Table 4). Crops grown under irrigated conditions also benefit from CO_2-induced decreases in crop stomatal conductance. For example, CWP of irrigated wheat in arid areas—covering 63% of harvested areas—increases by a median 18% (Supplementary Table 3). These beneficial effects on CWP reduce overall consumptive crop water use with non-negligible reductions in consumptive irrigation water use, which can be critical, as such use directly competes for water resources with other uses such as households, industry and the maintenance of other ecosystem services (Supplementary Table 5).

We then examine the contribution of simulated CO_2 effects on crop behaviour across regions by comparing CC w/ CO_2 and CC w/o CO_2 simulations. We find particularly larger effects on maize grown in semi-arid regions, including most of southern Africa, the Middle East and parts of central Asia, western USA and the Iberian Peninsula (Fig. 3a). Our results for maize exhibit a high level of confidence in the spatial distribution—except for the Iberian Peninsula, where a particularly large response simulated by some

Table 1 | Relative change in global average yield, AET and CWP (%), median values across all GCM–GGCM combinations for CC w/ CO_2 and CC w/o CO_2 simulations for 2080 relative to 2000 under RCP 8.5.

	Yield		AET		CWP	
	CC w/ CO_2	CC w/o CO_2	CC w/ CO_2	CC w/o CO_2	CC w/ CO_2	CC w/o CO_2
Maize	−8.5[−16.4;1]†	−21.2[−28.2;−13.3]*	−17.4[−23.7;−4.9]*	−8.2[−13.1;−1.6]†	13[2.8;22.4]‡	−12.9[−22.1;−1.9]*
Rice	−2.9[−12.3;13.8]	−27.2[−32.9;−16.3]*	−3.3[−19.8;−2.1]†	−3.3[−11.1;−0.1]†	9.7[−0.4;47]‡	−23[−27;−16.8]*
Soybean	0[−12.1;33.3]	−35.3[−40.5;−27.7]*	−8.3[−20.4;3.4]†	−4.7[−16.8;0.9]†	18.2[−8.7;41.8]‡	−26.2[−39.8;−18.8]*
Wheat	3.2[−0.6;13.7]‡	−22.6[−27.8;−14.9]*	−11[−20.8;−5.8]*	−6.6[−12.1;−4.8]*	27.2[6.6;37.2]§	−16.6[−23.6;−1.1]*

Numbers in square brackets are the first and third quartiles, respectively. Degree of agreement in the sign of change is characterized by the symbol (*: more than 80% agreement in a net decrease; †: between 60 and 80% agreement in a net decrease; ‡: between 60 and 80% agreement in a net increase; §: >80% agreement in a net increase; no symbol: <60% agreement in the sign of change).

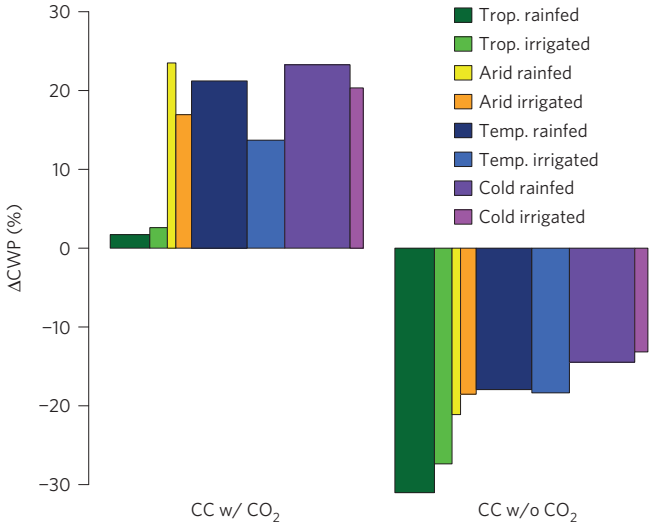

Figure 2 | Simulated CWP responses across agro-climatic regions. The median change in rainfed and irrigated CWP (%) in tropical (trop.), arid, temperate (temp.) and cold regions simulated under RCP 8.5 by 2080 relative to 2000 for all crops—GGCMs–GCMs combinations for CC w/ CO_2 and CC w/o CO_2 only. The width of the boxes varies according to corresponding total crop irrigated and rainfed harvested areas.

GGCMs increases the range of results (Supplementary Fig. 5a and Supplementary Results). In the case of the C_3 crops, we find the spatial distribution of CO_2 effects follows different patterns than for maize: for wheat (Fig. 3b), median simulated effects on CWP are relatively larger in tropical areas (20–30%) than in temperate areas (10–20%). For soybean and rice, we find smaller regional differences in the CO_2 effects, with overall larger effects for soybean (Fig. 3c,d). Furthermore, we find some regions show a particularly wide range of impacts across the simulation ensemble: notably western sub-Saharan Africa and eastern Brazil for rice (Supplementary Fig. 5c); the Middle East, southern Africa, southeast Asia and southwestern Australia for soybean (Supplementary Fig. 5d). Further information is presented in the Methods and supported by maps of individual model responses (Supplementary Figs 8–11).

Although results from the simulation ensemble confirm that the median CWP of six models generally agrees with observations (Fig. 1 and Supplementary Fig. 4), there are considerable variations among the models caused by differences in calibration and parameterization methods. The inclusion of six GGCMs in our modelling intercomparison study drastically amplifies the range of simulated CWP under CC w/ CO_2 (Fig. 4), which more than doubles by 2050 (the range is ±14% for an ensemble of 6 GGCMs × 1 GCM instead of ±6% for an ensemble of 1 GGCM × 5 GCMs). This is caused primarily by GGCMs differences in simulating crop response to CO_2 (Supplementary Table 6). We are able to differentiate the role of CO_2 from that of climate by quantifying uncertainties under both scenarios CC w/ CO_2 and CC w/o CO_2: we find the range in simulated global CWP reaches ±25% under CC w/ CO_2 instead of ±12% under CC w/o CO_2 (Supplementary Table 6; estimates refer to the median absolute deviation from the median). We therefore find a significantly larger variance resulting from multiple GGCM responses than from multiple bias-corrected GCM signals (Supplementary Fig. 7).

Our analysis provides a global spatially explicit assessment of the role of rising CO_2 on CWP throughout the twenty-first century, and explores variations in key mechanisms across agroclimatic regions. We show large regional differences in the intensity of CO_2 effects across the world (Figs 2 and 3) and between crop types (Figs 3 and 4). We find the range of simulated results (yield, AET, CWP) is comparable to the range of FACE measurements (Fig. 1 and Supplementary Fig. 4), which can vary widely from year to year and site to site[1], even though the sample of available CWP data

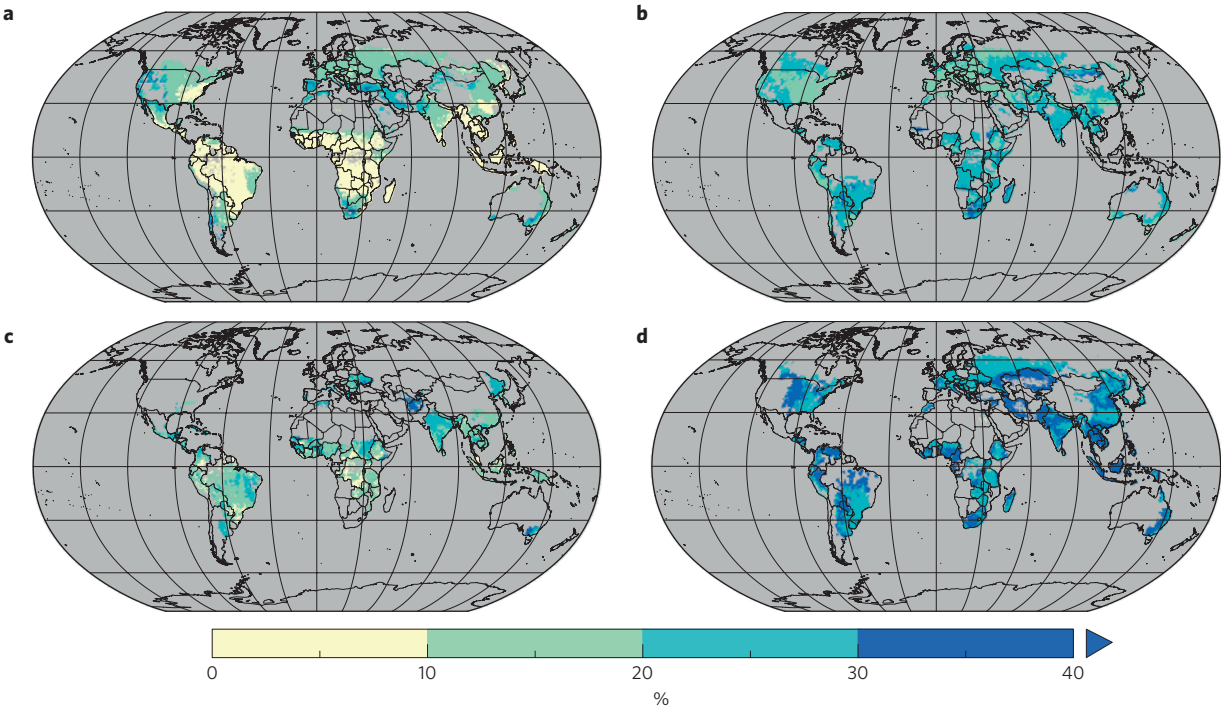

Figure 3 | Maps of median relative change between simulated CWP CC w/ CO_2 and CC w/o CO_2 only (%) in the model ensemble (including six GGCMs × five GCMs) by 2050 under RCP 8.5. Rainfed simulations are shown for maize (**a**), wheat (**b**), rice (**c**) and soybean (**d**). Simulated areas are masked by current rainfed areas from the MIRCA data set.

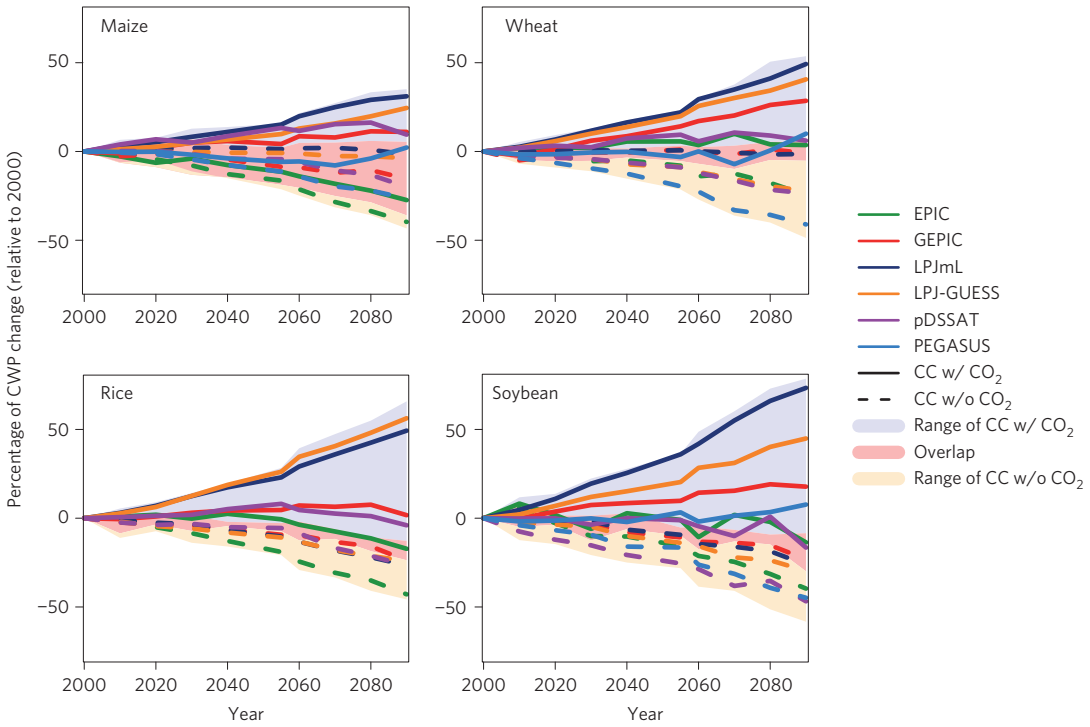

Figure 4 | Global average CWP (%) relative to 2000 simulated under RCP 8.5 for each GGCM driven by five different GCMs. Solid lines show median CWP under both climate change and CO_2 effects, whereas dashed lines show median CWP under climate change effects only—that is, with constant [CO_2]. Shaded areas show the range across the GGCM–GCM ensemble under CC w/o CO_2 (yellow) and CC w/ CO_2 (blue), distinctively, and overlap between CC w/o CO_2 and CC w/ CO_2 (red).

is very small. These FACE experiments are at present available in only a small number of locations (Arizona, USA, Germany and Australia for wheat; Japan and China for rice; Germany for maize; and Illinois, USA, for soybean). It is also important to highlight additional caveats in our evaluation. First, methods to represent CO_2 effects in GGCMs include a key assumption that crop responses to elevated [CO_2] will be the same under extremes of temperature and water supply as they are in the moderate conditions where experiments have been performed so far. Second, we compare current climate w/ and w/o CO_2 (FACE) with future climate w/ and w/o CO_2 (simulations). Third, simulation of irrigated systems can differ from actual irrigated systems in FACE (Methods). The dearth of long-term observational data and the large spread among model simulations highlights the urgent need for expanding FACE experiments, especially in arid and semi-arid cropland areas. Continuing coordinated efforts for model intercomparison and improvement are equally important. Finally, the use of GGCMs here could inform the design of subsequent FACE experiments to be conducted under more extreme growing conditions.

Our results—based on state-of-the-art modelling and observational capacities—demonstrate that a robust understanding of the role of rising [CO_2] is vital to assess potentially beneficial effects on crop production and agricultural water requirements; effects which might offer crucial opportunities for food and water security in arid and semi-arid areas[26,27]. Nonetheless, other sources of uncertainties in GGCMs have yet to be explored in greater detail, especially with respect to carbon–temperature–water–nitrogen interactions and agricultural management assumptions. We quantify the importance of CO_2 effects on potential water savings and, in so doing, highlight key limitations of global hydrological models that do not consider effects of CO_2 on ET[5,7]. The next generation of models needs to account for the large effects of elevated [CO_2] on crop water dynamics and global irrigation requirements. Anticipating climate impacts and interactions across the agriculture and water sectors is essential to improve the efficiency and resilience of agricultural systems. Food security, especially in arid and less developed regions, is not only a function of crop productivity and available land, but also of CWP and available water resources. This relationship is strongly affected by elevated [CO_2], and demands greater attention in scientific and policy assessment.

Methods

Methods and any associated references are available in the online version of the paper.

Received 15 June 2015; accepted 11 March 2016; published online 18 April 2016

References

1. Kimball, B. A. in *Handbook of Climate Change and Agroecosystems, Impacts, Adaptation, and Mitigation* Vol. 1 (eds Hillel, D. & Rosenzweig, C.) 87–107 (Imperial College, 2011).
2. Vanuytrecht, E., Raes, D., Willems, P. & Geerts, S. Quantifying field-scale effects of elevated carbon dioxide concentration on crops. *Clim. Res.* **54,** 35–47 (2012).
3. Rosenzweig, C. *et al*. Assessing agricultural risks of climate change in the 21st century in a global gridded crop model intercomparison. *Proc. Natl Acad. Sci. USA* **111,** 3268–3273 (2014).
4. Vörösmarty, C. J. *et al*. Global threats to human water security and river biodiversity. *Nature* **467,** 555–561 (2010).
5. Schewe, J. *et al*. Multimodel assessment of water scarcity under climate change. *Proc. Natl Acad. Sci. USA* **111,** 3245–3250 (2014).
6. Wheeler, T. R. & von Braun, J. Climate change impacts on global food security. *Science* **341,** 508–513 (2013).
7. Elliott, J. *et al*. Constraints and potentials of future irrigation water availability on agricultural production under climate change. *Proc. Natl Acad. Sci. USA* **111,** 3239–3244 (2014).
8. Hanjra, M. A. & Qureshi, M. E. Global water crisis and future food security in an era of climate change. *Food Policy* **35,** 365–377 (2010).

9. Rockström, J. & Falkenmark, M. Semiarid crop production from a hydrological perspective: gap between potential and actual yields. *Crit. Rev. Plant Sci.* **19,** 319–346 (2000).
10. Brauman, K. A., Siebert, S. & Foley, J. A. Improvements in crop water productivity increase water sustainability and food security—a global analysis. *Environ. Res. Lett.* **8,** 024030 (2013).
11. Burkart, S., Manderscheid, R., Wittich, K. P., Löpmeier, F. J. & Weigel, H. J. Elevated CO_2 effects on canopy and soil water flux parameters measured using a large chamber in crops grown with free-air CO_2 enrichment. *Plant Biol.* **13,** 258–269 (2011).
12. Long, S. P., Ainsworth, E. A., Leakey, A. D. B., Nösbsrger, J. & Ort, D. R. Food for thought: lower-than-expected crop yield stimulation with rising CO_2 concentrations. *Science* **312,** 1918–1921 (2006).
13. Tubiello, F. N. *et al*. Crop response to elevated CO_2 and world food supply: a comment on "Food for Thought..." by Long et al., Science 312: 1918–1921, 2006. *Eur. J. Agron.* **26,** 215–223 (2007).
14. Ainsworth, E. A., Leakey, A. D. B., Ort, D. R. & Long, S. P. FACE-ing the facts: inconsistencies and interdependence among field, chamber and modeling studies of elevated [CO_2] impacts on crop yield and food supply. *New Phytol.* **179,** 5–9 (2008).
15. Leakey, A. D. B. *et al*. Elevated CO_2 effects on plant carbon, nitrogen, and water relations: six important lessons from FACE. *J. Exp. Bot.* **60,** 2859–2876 (2009).
16. Leakey, A. D. B., Bishop, K. A. & Ainsworth, E. A. A multi-biome gap in understanding of crop and ecosystem responses to elevated CO_2. *Curr. Opin. Plant Biol.* **15,** 228–236 (2012).
17. Rosenthal, D. M. & Tomeo, N. J. Climate, crops and lacking data underlie regional disparities in the CO_2 fertilization effect. *Environ. Res. Lett.* **8,** 031001 (2013).
18. Boote, K. J., Jones, J. W., White, J. W., Asseng, S. & Lizaso, J. I. Putting mechanisms into crop production models. *Plant Cell Environ.* **36,** 1658–1672 (2013).
19. Liu, J. A GIS-based tool for modelling large-scale crop-water relations. *Environ. Modell. Softw.* **24,** 411–422 (2009).
20. Fader, M., Rost, S., Müller, C., Bondeau, A. & Gerten, D. Virtual water content of temperate cereals and maize: present and potential future patterns. *J. Hydrol.* **384,** 218–231 (2010).
21. Porter, J. R. *et al*. in *Climate Change 2014: Impacts, Adaptation, and Vulnerability* (eds Field, C. B. *et al*.) Ch. 7, 485–533 (IPCC, Cambridge Univ. Press, 2014).
22. Asseng, S. *et al*. Uncertainty in simulating wheat yields under climate change. *Nature Clim. Change* **3,** 827–832 (2013).
23. Hempel, S., Frieler, K., Warszawski, L., Schewe, J. & Piontek, F. A trend-preserving bias correction—the ISI-MIP approach. *Earth Syst. Dyn. Discuss.* **4,** 49–92 (2013).
24. Moss, R. H. *et al*. The next generation of scenarios for climate change research and assessment. *Nature* **463,** 747–756 (2010).
25. Portmann, F. T., Siebert, S. & Döll, P. MIRCA2000—Global monthly irrigated and rainfed crop areas around the year 2000: a new high-resolution data set for agricultural and hydrological modeling. *Glob. Biogeochem.* **24,** 024023 (2010).
26. Rockström, J. *et al*. Managing water in rainfed agriculture—The need for a paradigm shift. *Agric. Water Manage.* **97,** 543–550 (2010).
27. Rost, S. *et al*. Global potential to increase crop production through water management in rainfed agriculture. *Environ. Res. Lett.* **4,** 044002 (2009).

Acknowledgements

This work has been conducted under the framework of ISI-MIP and in partnership with the AgMIP community. The ISI-MIP Fast Track project was funded by the German Federal Ministry of Education and Research (BMBF) with project funding reference number 01LS1201A. We acknowledge the World Climate Research Programme's Working Group on Coupled Modelling, which is responsible for CMIP, and we thank the climate modelling groups for producing and making available their model output. For CMIP the US Department of Energy's Program for Climate Model Diagnosis and Intercomparison provides coordinating support and led development of software infrastructure in partnership with the Global Organization for Earth System Science Portals. This work was also supported by a research stipend from the Tyndall Centre for Climate Change Research and a Belmont Forum grant from the UK Natural Environment Research Council (grant no. NE/L008785/1) to D.D., by the National Science Foundation under grants SBE-0951576 and GEO-1215910 to J.E., by the BMBF grant 01LN1317A to C.M., and by the Formas Strong Research Environment 'land use today and tomorrow' to S.O., T.A.M.P. was supported by EU FP7 project EMBRACE (grant no. 282672). We are grateful to B. A. Kimball and A. Leakey for pointing out appropriate literature on the FACE experiments.

Author contributions

D.D. had the main responsibility for the study idea, methods, analysis and writing the paper. D.D., J.E. and C.R. designed and coordinated the modelling intercomparison analysis. J.E., C.F., C.M. and T.A.M.P. contributed to analysis. D.D., J.E., C.F., C.M., T.A.M.P., S.O., N.K. and E.S. performed the crop model simulations. J.E., C.M., C.F., T.A.M.P., K.J.B., D.C. and A.C.R. made significant contributions in developing the paper structure and interpreting the results. J.E., A.C.R., D.G., S.S., H.Y., J.W.J. and C.R. made important contributions in developing the original study idea. All authors contributed to writing the paper.

Additional information

Supplementary information is available in the online version of the paper. Reprints and permissions information is available online at www.nature.com/reprints. Correspondence and requests for materials should be addressed to D.D.

Competing financial interests

The authors declare no competing financial interests.

Methods

Overview of the global gridded crop models. The model ensemble comprises six global gridded crop models (GGCMs) driven by daily climate data from five different global climate models (GCMs) under RCP 8.5 (ref. 3). The six GGCMs consist of:

1. the Environmental Policy Integrated Climate (EPIC) model[28,29] (originally the Erosion Productivity Impact Calculator; ref. 30).
2. the Geographic Information System-based Environmental Policy Integrated Climate (GEPIC) model[30–32].
3. the Lund-Potsdam-Jena managed Land (LPJmL) dynamic global vegetation and water balance model[20,33,34].
4. the Lund-Potsdam-Jena General Ecosystem Simulator (LPJ-GUESS) with managed land[33,35,36].
5. the parallel Decision Support System for Agro-technology Transfer (pDSSAT[37,38]; using the Crop Environment Resource Synthesis (CERES) models for maize, wheat, and rice and the Crop Template approach (CROPGRO) for soybean).
6. the Predicting Ecosystem Goods And Services Using Scenarios (PEGASUS) model[39,40].

These GGCMs can be grouped into two families spanning more than three decades of model development:

- site-based crop models—extended for global analyses using a geographical information system (EPIC and GEPIC) and an advanced parallel simulation system (pDSSAT).
- ecosystem models—initially developed to simulate the terrestrial carbon cycle for natural vegetation using downscaled global climate data and then extended to represent managed land (LPJmL, LPJ-GUESS and PEGASUS).

The site-based crop models tend to include a more detailed representation of cropping systems but necessitate substantial computing resources, whereas the ecosystem models typically include less detail on crop management but present the advantage of being run globally in a short fraction of time. In addition, because the ecosystem models simulate global carbon and water cycles, they are useful tools for assessing crop production in the context of global environmental change.

Model representation of biophysical processes. Biophysical processes represented in GGCMs include light utilization, CO_2 effects (see next section for CO_2), environmental stresses, soil water dynamic and, for some, soil nutrient cycling. First, photosynthesis is described with either a simple radiation use efficiency (RUE) (for example, PEGASUS, described in ref. 40) or a detailed leaf-level photosynthesis respiration (PR) (ref. 41) (for example, LPJmL and LPJ-GUESS, described in ref. 42) approach. Representation of CO_2 fertilization effects on photosynthesis and transpiration rates thus follows either a descriptive (RUE-type models) or explanatory approach (PR-type models). Second, all GGCMs take into account temperature and water stress. Most models also include nitrogen stress (except the LPJ-type models). In addition, both EPIC-type models represent aluminium and oxygen stresses. PEGASUS represents heat stress effect at anthesis[38], resulting in systematically strongest negative impacts (Supplementary Fig. 1). Third, GGCMs differ in respect to crop water demand and estimated evapotranspiration (ET): the EPIC-type models use the Penman–Monteith approach[43,44], whereas the other GGCMs use the Priestley–Taylor approach[45]. In addition, the number of soil layers varies among GGCMs and roots are either linearly or exponentially distributed throughout the soil depth. Finally, crop phenology in GGCMs depends on temperature using growing degree-day accumulation, which varies with models' definition of base and maximum temperature thresholds that are also crop specific (see Supplementary Table 3 in ref. 3 (accessible at http://www.pnas.org/content/suppl/2013/12/16/1222463110.DCSupplemental/sapp.pdf)).

Model representation and parameterization of crop response to $[CO_2]$. The choice of light utilization representation method (RUE versus PR) in GGCM determines that of CO_2 effects. In the RUE approach (followed by PEGASUS, EPIC, GEPIC and pDSSAT—for wheat/rice/maize), rising $[CO_2]$ increases a RUE coefficient, which proportionally affects the rate of photosynthesis[31,46]. In PEGASUS, parameterization of the modified RUE coefficient was done by comparing grid-cell simulations and FACE results reported in ref. 12 using $[CO_2]$ levels of 380 ppm for the baseline[39]. In EPIC and GEPIC, parameterization of the modified RUE coefficient uses pre-FACE data normalized around 330 ppm, as described in ref. 47. In the case of pDSSAT, Boote *et al.* (ref. 48) evaluated the CO_2-responses of each DSSAT model, which was originally based on pre-FACE observations and normalized to 330 ppm. Evaluations for CERES-wheat and rice showed that the simulated responses to doubled CO_2 (27 and 32% response for wheat and rice, respectively) were sufficiently close to reported FACE data (31 and 30% response for wheat and rice, respectively). The review by Boote *et al.* (ref. 48) concluded that prior DSSAT parameterization to CO_2 effect for C_4 CERES-Maize, Sorghum, and Millet models was too high (based on old literature). Therefore, the response of these three C_4 crops in DSSAT was reduced to give a 4.2% grain yield increase for doubled CO_2 (350 to 700 ppm) beginning with DSSAT version V4.5 released in 2010, and in this study.

Transpiration in PEGASUS, EPIC and GEPIC increases with CO_2, following a logarithmic equation as in refs 31,46, and is identical for all crops[39]. Transpiration in pDSSAT follows the approach of leaf resistance, increasing as a function of rising CO_2—one equation for C_3 and one for C_4. Then, the daily transpiration is reduced as a function of rising CO_2, where the relative transpiration effect ratio is computed in a Penman–Monteith-style equation that considers the psychrometric constant, gamma, the two canopy resistances (at reference CO_2 and at present CO_2), and boundary resistance. The effect is modest, and has not been tested with any transpiration data (see ref. 48 for more information).

The PR approach in pDSSAT-soybean (that is, CROPGRO-soybean) uses an analytical derivation, for example, RuBP-limiting side of the rubisco kinetics of ref. 49, as described in refs 50,51. Farquhar and von Caemmerer (ref. 49) developed an analytical solution for quantum efficiency that depends on the RuBP-limiting (light-limiting) phase, with no need to consider rubisco enzyme parameters. The approach is applied to make quantum efficiency and light-saturated photosynthesis (Amax) sensitive to temperature and CO_2 within asymptotic exponential equations for sunlit and shaded leaf classes. As a replacement for rubisco enzyme, the Amax term is strongly dependent on specific leaf nitrogen. The CO_2 response for soybean is an emergent outcome of this parameterization and was shown to give yield response to doubled CO_2 comparable to metadata[48]. Similarly, in the PR approach followed by the two LPJ models, potential photosynthesis rate is calculated as a function of co-limitation by light and the rubisco enzyme, considering the influences of photosynthetically active radiation, temperature and $[CO_2]$[42]. Note that, although rubisco capacity is not prescribed but maximized daily, photosynthesis rate is not acclimated in response to a possible downregulation of rubisco activity at elevated $[CO_2]$. In case of a soil moisture deficit, both photosynthesis and transpiration (canopy conductance) are reduced nonlinearly[52].

Model representation of agricultural management practices. Representation of farm management practices is also a source of difference in GGCM results: whether and how fertilizer application, irrigation, crop residue management, crop cultivar selection and planting date decision are simulated strongly influence yield and other outputs. The site-specific models (that is, EPIC, GEPIC and pDSSAT) apply fertilizer dynamically through the crop growing season: application occurs at specific stages of the crop development to take into account the role of both application quantity and timing. PEGASUS applies fertilizer as a daily stress function and thus does not simulate effect of fertilizer application timing[39]. LPJmL and LPJ-GUESS do not represent fertilizer application. Also, although ISI-MIP provided harmonized climate data, models generally used differing input data/methods for soil characteristics and national fertilizer application rates[3].

Planting date decision and choice of crop cultivars also vary among GGCMs. Supplementary Tables 2 and 4 in ref. 3 provide a detailed description of GGCMs assumptions (accessible at http://www.pnas.org/content/suppl/2013/12/16/1222463110.DCSupplemental/sapp.pdf). Chiefly, PEGASUS and GEPIC allow for adaptation in planting window whereas the other GGCMs assumed planting window fixed to present day. LPJ-GUESS and PEGASUS also allow for adaptation in crop cultivars (growing degree-day requirements) whereas the other GGCMs use fixed crop cultivars.

Model calibration. Finally, GGCM calibration methods differ significantly between site-specific and ecosystem models. Ecosystem models are calibrated to global crop yield data (for example, PEGASUS, ref. 39) and FAO national statistics (for example, LPJmL, ref. 33) by tuning a limited number of parameters, whereas the site-specific models use a large set of parameters previously calibrated at various study sites[3]. Given all these differences, we found models from similar origins, such as EPIC/GEPIC and LPJmL/LPJ-GUESS differ enough to be considered each as an independent GGCM within the ensemble.

Climate inputs. All GGCMs were run at 0.5° latitude × 0.5° longitude spatial resolution using bias-corrected climate scenarios resulting from five GCMs under RCP 8.5 for the period 1971–2099. Hempel *et al.* (ref. 23) provides a detailed description of the GCMs used and downscaling methods. The five GCMs include:

1. HadGEM2-ES (developed at the Hadley Centre for Climate Prediction and Research in the UK).
2. IPSL-CM5A-LR (developed at the Institut Pierre Simon Laplace in France).
3. MIROC-ESM-CHEM (cooperatively developed at the Center for the University of Tokyo, the National Institute for Environmental Studies, and the Frontier Research Center for Global Change in Japan).
4. GFDL-ESM2M (developed at the Geophysical Fluid Dynamics Laboratory in the United States).
5. NorESM1-M (developed at the Norwegian Climate Centre in Norway).

Modelling protocol. All GGCMs simulated maize, wheat, rice and soybean except PEGASUS, which does not simulate rice. In the case of wheat, PEGASUS simulated spring variety everywhere, as it does not simulate winter wheat, assuming a spring variety was planted in areas where a winter variety is typically grown. Each GGCM–GCM combination was run with (w/) and without (w/o) CO_2 from 1971 to 2099 according to the modelling protocol developed within the framework of the Agricultural Model Intercomparison and Improvement Project (AgMIP) and the Inter-Sectoral Impacts Model Intercomparison Project (ISI-MIP)[3]. In the CC w/o CO_2 simulations, [CO_2] were kept constant to 380 ppm, corresponding to concentrations in the year 2000. For this analysis, simulations under CC w/o CO_2 have been updated from the original set of simulations presented in ref. 3 to ensure all models used the same [CO_2] baseline—that is, 380 ppm in 2000. We analyse GGCM outputs of crop yield and AET and calculate crop water productivity (CWP in kg m^{-3}) for a specific year following the equation: CWP = 100Y/AET where Y is the crop yield in ton ha^{-1} yr^{-1} and AET is the total actual evapotranspiration in mm over the growing season of that specific year. Each year of crop yield data is averaged over a 30-year or a 10-year period according to the ISI-MIP protocol. GGCMs perform simulations over the entire land surface according to their own agroclimatic suitability indices. We then mask out results to current cropland rainfed and irrigated areas using the MIRCA data set[25]. Global average estimates of yield, AET and CWP consist in weighted mean values across all grid cells, weighted by crop rainfed and irrigated harvested areas. Two irrigation scenarios were considered: no irrigation (that is, rainfed) and fully irrigated assuming no water stress (the specific threshold for water stress was independently selected by each GGCM modelling team). We calculate global average CWP from actual yield combining both fully irrigated and rainfed yields according to the MIRCA data for irrigated cropland areas[25]. We further disaggregated our results by climatic regions, following the Köppen–Geiger system to distinguish between tropical, arid, temperate and cold regions[53]. An extensive description of the GGCMs that participated in the AgMIP/ISI-MIP fast-track exercise is also published in the Supplementary Appendix of ref. 3.

Comparison to FACE observations. To assess the performance of GGCMs against current observations, we compiled available results from FACE experiments reporting on CWP identified at several locations across the world (wheat in Arizona, USA[54–57], Germany[11,58] and Australia[59]; rice in China[60] and Japan[61]; soybean in Illinois, USA[62]; and maize in Germany[63]). Supplementary Tables 1 and 2 summarize FACE site characteristics and GGCMs results. We compared GGCM simulations against these FACE observations (that is, at the grid-cell level) for rainfed and/or irrigated conditions (Supplementary Tables 1 and 2). We selected corresponding yield and AET values from the GGCM simulations at grid cells matching the coordinates of FACE observations to calculate the relative change in CWP between CC w/ CO_2 and CC w/o CO_2. Ambient atmospheric [CO_2] in the FACE experiments varied between 360 and 380 ppm and elevated CO_2 corresponds to 550 ppm. We thus used 10-year average estimates around the year 2050, which corresponds to the same increment of [CO_2] level rise relative to the baseline (550 ppm in 2050 to 380 ppm in 2000, respectively). In most FACE experiments reported here, temperatures are held constant. We thus estimate the relative change between w/ and w/o CO_2 around the year 2050 to single out effects of CO_2 from those of temperature and precipitation changes relative to the year 2000.

Sources of differences in simulated CWP. Model evaluation against FACE measurements show median simulated CO_2 effects on CWP tend to be slightly greater than observation for maize (Fig. 1 and Supplementary Fig. 1) owing to stronger simulated effects on ET (Supplementary Fig. 3). Overall, we find CO_2 effects on maize yield are minimal for both simulated and observed data (Supplementary Fig. 2). However, the choice of a descriptive rather than explanatory representation of light utilization (that is, radiation use efficiency—RUE—versus leaf-level photosynthesis and respiration—PR; see Methods) slightly overestimates the CO_2 effects on maize yield at the 'wet' FACE site (Supplementary Fig. 2), and thus partly contributes to greater simulated CO_2 effects on CWP in the ensemble (Fig. 1). In contrast, in drier agroclimatic conditions, the greater responsiveness of crop yield and CWP to elevated [CO_2] appears independent of the choice of light utilization representation method but rather sensitive to model calibration and parameterization method (Supplementary Fig. 8).

In the case of the C_3 crops, we find simulated CO_2 effects are much stronger on carbon assimilation and thus on leaf area and crop yield in all models, broadly confirming FACE measurements (Fig. 1). However, CO_2 responses is much higher when simulated using the PR approach to light utilization representation. We find simulated CO_2 effects on CWP tend to be slightly lower than observations for wheat and rice and nearly the same as observations for soybean (Fig. 1 and Supplementary Table 1). Differences in assumptions of fertilizer input is the main source of differences in simulated wheat and rice responses to elevated [CO_2]: for example, EPIC, which considers high nitrogen (N) application rates everywhere, shows much stronger positive effects of elevated [CO_2] in Africa than GEPIC, which applies N inputs only according to present-day levels; similarly, LPJmL is tuned—partly through a constraint in the maximum leaf area index (LAI)—to FAO yields, and thus indirectly accounts for different nutrient/management intensity across nations. LPJmL thus simulates a lower CWP response in many parts of Africa and in low-N-inputs regions, unlike LPJ-GUESS, which does not have a constraint on the maximum LAI and can thus reach higher AET values without a corresponding increase in yield (Supplementary Figs 9–11). We also find these differences lessen for soybean because, being an N-fixing legume, it is less sensitive to N input levels. Finally, EPIC, which in this study constrains irrigation water use, shows smaller CO_2 effects on AET than GEPIC, which allows for optimum irrigation water use (Supplementary Fig. 3). Furthermore, the choice of ET equation, which differs between the EPIC-type models and pDSSAT and PEGASUS (ref. 3), contributes to important differences in model behaviour in some regions (Supplementary Figs 9–11). Another source of difference between LPJmL and LPJ-GUESS concerns model assumption on the choice of crop cultivar, which affects timing of the growing. As a consequence, allocation of biomass production over the growing period differs in these two models. Similarly, GEPIC and EPIC use different assumptions on planting date decision, which is also a source of differences in simulated yield and AET.

References

28. Gassman, P. W. *et al*. *Historical Development and Applications of the EPIC and APEX Models* Working Paper 05-WP 397 (2005); http://www.card.iastate.edu/publications/dbs/pdffiles/05wp397.pdf
29. Izaurralde, R. C., Williams, J. R., McGill, W. B., Rosenberg, N. J. & Jakas, M. C. Q. Simulating soil C dynamics with EPIC: model description and testing against long-term data. *Ecol. Model.* **192,** 362–384 (2006).
30. Williams, J. R. *EPIC-Erosion/Productivity Impact Calculator* Technical Bulletin Number 1768 (USDA Agricultural Research Service, 1990).
31. Williams, J. R. in *Computer Models of Watershed Hydrology* (ed. Singh, V. P.) Ch. 25, 909–1000 (Water Resources, 1995).
32. Liu, J., Williams, J. R., Zehnder, A. & Yang, H. GEPIC—modelling wheat yield and crop water productivity with high resolution on a global scale. *Agric. Syst.* **94,** 478–493 (2007).
33. Bondeau, A. *et al*. Modelling the role of agriculture in the 20th century global terrestrial carbon balance. *Glob. Change Biol.* **13,** 679–706 (2007).
34. Waha, K., van Bussel, L. G. J., Müller, C. & Bondeau, A. Climate-driven simulation of global crop sowing dates. *Glob. Ecol. Biogeogr.* **21,** 247–259 (2011).
35. Lindeskog, M. *et al*. Implications of accounting for land use in simulations of ecosystem services and carbon cycling in Africa. *Earth Syst. Dyn. Discuss.* **4,** 235–278 (2013).
36. Smith, B., Prentice, I. C. & Sykes, M. T. Representation of vegetation dynamics in the modelling of terrestrial ecosystems: comparing two contrasting approaches within European climate space. *Glob. Ecol. Biogeogr.* **10,** 621–637 (2001).
37. Elliott, J. *et al*. The parallel system for integrating impact models and sectors (pSIMS). *Environ. Modell. Softw.* **62,** 509–516 (2014).
38. Jones, J. W. *et al*. The DSSAT cropping system model. *Eur. J. Agron.* **18,** 235–265 (2003).
39. Deryng, D., Conway, D., Ramankutty, N., Price, J. & Warren, R. Global crop yield response to extreme heat stress under multiple climate change futures. *Environ. Res. Lett.* **9,** 034011 (2014).
40. Deryng, D., Sacks, W. J., Barford, C. C. & Ramankutty, N. Simulating the effects of climate and agricultural management practices on global crop yield. *Glob. Biogeochem. Cycles* **25,** 1–18 (2011).
41. Farquhar, G. D., Caemmerer, S. & Berry, J. A. A biochemical model of photosynthetic CO_2 assimilation in leaves of C_3 species. *Planta* **149,** 78–90 (1980).
42. Sitch, S. *et al*. Evaluation of ecosystem dynamics, plant geography and terrestrial carbon cycling inthe LPJ dynamic global vegetation model. *Glob. Change Biol.* **9,** 161–185 (2003).
43. Penman, H. L. Natural evaporation from open water, bare soil, and grass. *Proc. R. Soc. Lond. A* **193,** 120–145 (1948).
44. Monteith, J. Evaporation and environment. *Symp. Soc. Exp. Biol.* **19,** 205–224 (1965).
45. Priestley, C. H. B. & Taylor, R. J. On the assessment of surface heat flux and evaporation using large-scale parameters. *Mon. Weath. Rev.* **100,** 81–92 (1972).
46. Neitsch, S. L., Arnold, J. G., Kiniry, J. R. & Williams, J. R. *Soil and Water Assessment Tool. Theoretical Documentation, Version 2005* (Grassland, Soil and Water Research Laboratory, Agricultural Research Service, 2005).
47. Stockle, C. O., Williams, J. R., Rosenberg, N. J. & Jones, C. A. A method for estimating the direct and climatic effects of rising atmospheric carbon dioxide on growth and yield of crops: Part 1–modification of the epic model for climate change analysis. *Agric. Syst.* **38,** 225–238 (1992).

48. Boote, K. J., Allen, L. H. Jr, Prasad, P. V. V. & Jones, J. W. in *Handbook of Climate Change and Agroecosystems—Impacts, Adaptation, and Mitigation* Vol. 1 (eds Hillel, D. & Rosenzweig, C.) Ch. 6 (Imperial College, 2011).
49. Farquhar, G. & von Caemmerer, S. in *Encyclopedia of Plant Physiology. New Series* Vol. 12B (ed. Lange, O.) 549–587 (Springer, 1982).
50. Boote, K. J. & Pickering, N. B. Modeling photosynthesis of row crop canopies. *HortScience* **29,** 1423–1434 (1994).
51. Pickering, N. B., Jones, J. W. & Boote, K. J. in *Climate Change and Agriculture: Analysis of Potential International Impacts* (eds Rosenzweig, C., Jones, J. W. & Allen, L. H. J.) 147–162 (American Society of Agronomy, 1995).
52. Gerten, D., Schaphoff, S. & Lucht, W. Potential future changes in water limitations of the terrestrial biosphere. *Climatic Change* **80,** 277–299 (2007).
53. Peel, M. C., Finlayson, B. L. & McMahon, T. A. Updated world map of the Köppen-Geiger climate classification. *Hydrol. Earth Syst. Sci.* **4,** 439–473 (2007).
54. Hunsaker, D. J., Kimball, B. A., Pinter, P. J., LaMorte, R. L. & Wall, G. W. Carbon dioxide enrichment and irrigation effects on wheat evapotranspiration and water use efficiency. *Trans. ASAE* **39,** 1345–1355 (1996).
55. Hunsaker, D. J. *et al*. CO_2 enrichment and soil nitrogen effects on wheat evapotranspiration and water use efficiency. *Agric. For. Meteorol.* **104,** 85–105 (2000).
56. Kimball, B. A., Kobayashi, K. & Bindi, M.*Responses of Agricultural Crops to Free-Air CO_2 Enrichment* **77,** 293–368 (2002).
57. Kimball, B. A. *et al*. Free-air CO_2 enrichment and soil nitrogen effects on energy balance and evapotranspiration of wheat. *Wat. Resour. Res.* **35,** 1179–1190 (1999).
58. Weigel, H.-J. & Manderscheid, R. Crop growth responses to free air CO_2 enrichment and nitrogen fertilization: rotating barley, ryegrass, sugar beet and wheat. *Eur. J. Agron.* **43,** 97–107 (2012).
59. O'Leary, G. *et al*. Response of wheat growth, grain yield and water use to elevated CO_2 under a Free-Air CO_2 Enrichment (FACE) experiment and modelling in a semi-arid environment. *Glob. Change Biol.* **21,** 2670–2686 (2015).
60. Zhu, C., Xu, X., Wang, D., Zhu, J. & Liu, G. An indica rice genotype showed a similar yield enhancement to that of hybrid rice under free air carbon dioxide enrichment. *Sci. Rep.* **5,** 12719 (2015).
61. Shimono, H., Nakamura, H., Hasegawa, T. & Okada, M. Lower responsiveness of canopy evapotranspiration rate than of leaf stomatal conductance to open-air CO_2 elevation in rice. *Glob. Change Biol.* **19,** 2444–2453 (2013).
62. Bernacchi, C. J., Kimball, B. A., Quarles, D. R., Long, S. P. & Ort, D. R. Decreases in stomatal conductance of soybean under open-air elevation of $[CO_2]$ are closely coupled with decreases in ecosystem evapotranspiration. *Plant Physiol.* **143,** 134–144 (2006).
63. Manderscheid, R., Erbs, M. & Weigel, H.-J. Interactive effects of free-air CO_2 enrichment and drought stress on maize growth. *Eur. J. Agron.* **52,** 11–21 (2014).